Yu et al. Journal of Orthopaedic Surgery and Research (2025) 20:348
https://doi.org/10.1186/s13018-025-05757-5

Journal of Orthopaedic Surgery and Research

RESEARCH

Open Access

Knotted single lasso loop has a lower stiffness and comparable ultimate failure strength compared with knotless whipstitch fixation in onlay tenodesis

Jiong Yu[1*], Jingyi Mi[1], Kai Huang[2] and Renfei Qi[2]

Abstract

Background Suture and knotless anchor onlay tenodesis are two common treatments for biceps lesions; however, there is a paucity of biomechanical studies evaluating the efficacy and structural integrity of these techniques.

Methods Tendons were harvested from four lower extremity fresh cadaver specimens, including the extensor digitorum longus, peroneus longus, peroneus brevis, and anterior tibialis tendons. Each tendon diameter was recorded using a digital Vernier caliper. Sixteen 3D printed proximal humeri models were allocated to either the single lasso loop with suture anchor (SLL) group or the whipstitch with knotless suture anchor (WSA) group. Each tenodesis model was initially tested on an electrodynamic material testing instrument under a cyclic load ranging from 5 to 70 N at a speed of 1.25 mm/s. The force on the tendon was then returned to 5 N, which was pulled until the ultimate failure of the construct. Displacement during cyclic loading, ultimate failure load, stiffness, and failure modes were assessed.

Results Fourteen tenodesis models were validated, and two models were discarded due to technical errors. No significant differences between the two groups were observed regarding tendon diameter, ultimate failure load, and displacement at ultimate failure load. However, the construct stiffness for the SLL group was lower than that of the WSA group (58.02 ± 5.62 N/mm vs. 72.24 ± 15.63 N/mm, $P = 0.043$).

Conclusion The SLL group had a lower construct stiffness than the WSA group, whereas construct displacement and ultimate failure load were similar in both groups. Therefore, SLL biceps tenodesis may offer a convenient alternative, with lower tendon migration fixation, while performing an arthroscopic biceps tenodesis.

Level of evidence Basic Science Study.

Keywords Biceps tenodesis, Onlay tenodesis, Long head of biceps tendon, Suture anchor, Knotless

*Correspondence:
Jiong Yu
ithiel.yu@icloud.com
[1]Department of Sports Medicine, Wuxi Ninth People's Hospital Affiliated to Soochow University, Liangxi Road, No 999, Binhu District, Wuxi, Jiangsu, China
[2]Orthopaedic Institute, Wuxi Ninth People's Hospital Affiliated to Soochow University, Wuxi, Jiangsu, China

Introduction

Biceps tenodesis is widely accepted as the optimal treatment for superior labral anterior–posterior (SLAP) lesions, especially for overhead throwing athletes [1–4]. Onlay tenodesis with a knotless suture anchor has a lower rate of postoperative Popeye deformity than inlay interference screw fixation [5]; however, extracorporeal suture preparation is often necessary for the arthroscopic knotless onlay tenodesis of the biceps tendon, which is technically demanding. A single lasso loop with suture anchor (SLL) for biceps tenodesis was introduced for rotator cuff repair [6]. It was later modified as a 360° lasso loop applied to the tenodesis area [7], which is more convenient as it requires no further tendon preparation for arthroscopic procedures. Although the lasso loop results in a higher ultimate failure load and stiffness, the 360° lasso loop can cut through the tendon more easily [7], which might be one of the reasons for postoperative Popeye deformity.

Human cadavers have been a reliable resource for biomechanical studies; however, a shortage of cadavers is not uncommon in China owing to the economic status of the region and cultural and religious factors [8, 9]. Three-dimensional (3D) printed models using polylactic acid (PLA) are a cheap and accessible alternative for biomechanical tests with promising applications in orthopedics studies [10]. Therefore, the current study aimed to investigate the biomechanical characters of two onlay biceps tenodesis techniques, SLL and whipstitch knotless suture anchor (WSA), using 14 3D printed PLA models with harvested tendons.

Methods

3D-printed proximal humerus and tendon Preparation

Following approval from our hospital's ethics committee, a 24-year-old healthy male volunteer (height: 168 cm; weight: 69 kg) with normal bilateral shoulder range of motion and no history of shoulder injury or deformity was recruited. After obtaining informed consent, computed tomography (CT) imaging (Somatom Definition Flash; Siemens Healthcare, Erlangen, Germany) was performed to capture data on his humerus, the upper extremity's largest bone. The proximal third of the humerus was segmented and converted into stereolithography (STL) format for 3D printing.

The design process utilized nTopology software for computer-aided design (CAD), creating a model with a 2.5 mm thick cortical shell and an internal gyroid infill structure at 22% density [11]. The gyroid pattern featured a 14 mm pitch and 1.5 mm wall thickness, balancing strength and material efficiency. Fabrication was conducted via fused deposition modeling (FDM) using polylactic acid (PLA) filament with the following properties: 1.75 mm diameter (tolerance: ±0.02–0.03 mm), density of 1.24–1.25 g/cm^3, tensile strength of 65 MPa, melting point of 160 °C, and shrinkage rate of 0.3%.

Printing was executed on an FDM printer (Black-Flame Inc., Shanghai, China)) preheated to 200 °C, with a layer height of 0.2 mm, extruder temperature of 190–220 °C, bed temperature of 50–60 °C, and print speed of 40–60 mm/s. The cortical shell was set at 2.5 mm, encasing the continuous gyroid infill. Post-processing included cooling to prevent deformation (given PLA's low heat resistance of ~52 °C), removal of supports, and sanding for a smooth finish.

Tendons were obtained from four fresh cadaver lower extremity specimens, specifically the extensor digitorum longus, peroneus longus, peroneus brevis, and anterior tibialis tendons. Each tendon was carefully harvested, and its diameter was measured with a digital Vernier caliper to ensure precision.

Surgical technique

After completion of the 3D-printed humerus model and tendon preparation, the tenodesis models were randomly assigned into SLL and WSA groups. A 4.5 mm suture was used in the SLL group (Biocomposite Corkscrew, Arthrex, Naples, FL), following the technique introduced by Lafosse [12]. Furthermore, a no. 2 fiberwire with five stitches for tendon preparation and a 4.75 mm knotless suture anchor (Biocomposite Swivelock, Arthrex, Naples, FL) [13] was used in the WSA group with the onlay technique [5]. A guidewire was placed 2–3 cm distal to the most proximal aspect of the bicipital groove, and perpendicular to the surface of the printed model.

Biomechanic testing

Following tenodesis, the tendon tissue was secured, using a custom soft tissue clamp, to the actuator of the dynamic testing machine (ElectroPuls E3000; Instron Systems), 5 cm proximal to the fixation site of the biceps tendon. The printed humerus was secured and clamped at the base of the dynamic testing machine, allowing the biceps to be pulled vertically along the longitudinal axis of the humeral shaft. Each tenodesis model was tested with the Instron E3000, with a preconditioning load of 5 N for 2 min, followed by 500 cyclic loads commencing from 5 to 70 N at a speed of 1.25 mm/s. The force on the tendon was then returned to 5 N, and the tendon was pulled until the ultimate failure of the construct. Tendons were kept moist by spraying with saline every 5 min. Displacement during the first cyclic load, 500th cyclic load, ultimate failure loads, and stiffness were recorded, and failure modes were assessed.

Statistical analysis

Based on our preliminary results of the ultimate failure load, the sample size was calculated using Power Analysis and Sample Size (PASS; version 21.0.3; NCSS, Kaysville, UT, USA) software. With a significance level (alpha) of 0.05, and using a two-sample unequal-variance t-test, two group sample sizes of seven achieved 80% power. Considering failures during the biomechanic test, we finally allocated 16 models, with eight models in each group. The Statistical Package for the Social Sciences (SPSS), version 26 (SPSS Inc., Chicago, IL, USA), was used for statistical analyses. Parametric data (tendon diameter, ultimate failure load, ultimate failure load displacement, and stiffness) between the groups were compared using the independent Student's t-test, and nonparametric data (first and 500th cyclic load displacements) were compared using the Mann–Whitney U test. Statistical significance was set at $P < 0.05$.

Results

The axial view of the internal pattern in the 3D printed humerus and the knotted onlay tenodesis model with the SLL anchor is shown in Fig. 1A and B. The diameter of the harvested tendon was measured using the Vernier caliper (Fig. 2). The setup for biomechanical testing is shown in Fig. 3. Two models were excluded for the following technical reasons: one, the printed humerus model was inadequately secured to the actuator base, resulting in loose fixation and significant errors in the cyclic load-displacement measurements, and the other model was securely fixed but the cyclic load was tilted away from the humerus axis. Data analyses were performed on the remaining 14 models. The mean diameter of the harvested tendons was 6.35 ± 0.84 mm and 6.49 ± 0.64 mm ($P = 0.73$), the first cyclic load displacement was 6.02 ± 3.23 mm and 4.61 ± 1.27 mm ($P = 0.41$), and the 500th cyclic load displacement was 9.66 ± 3.39 mm and 9.61 ± 4.14 mm ($P = 0.80$) in the SLL and WSA group, respectively. The ultimate failure load was 191.43 ± 42.59 N in the SLL group and 188.57 ± 50.14 N in the WSA group ($P = 0.37$), while the ultimate failure displacement was 14.66 ± 4.70 mm in the SLL group and 16.58 ± 4.09 mm in the WSA group ($P = 0.91$). The stiffness was found to be 58.02 ± 5.62 N/mm and 72.24 ± 15.63 N/mm ($P = 0.043$) in the SLL and WSA groups, respectively (Table 1).

Regarding the failure mode in the SLL group, a knot breakout event was observed in one model (Video 1). The other models showed no apparent tenodesis breakout events (Fig. 4A). Tendons migrated from the original site by either gradual suture pulling from the construct or elongated sutures in the WSA group models (Fig. 4B and Video 2).

Discussion

Our study demonstrated that the SLL technique exhibited lower construct stiffness compared to the WSA technique (58.02 ± 5.62 N/mm vs. 72.24 ± 15.63 N/mm, $p = 0.043$). However, no significant differences were observed in terms of ultimate failure load, displacement at ultimate failure, or tendon diameter between the two

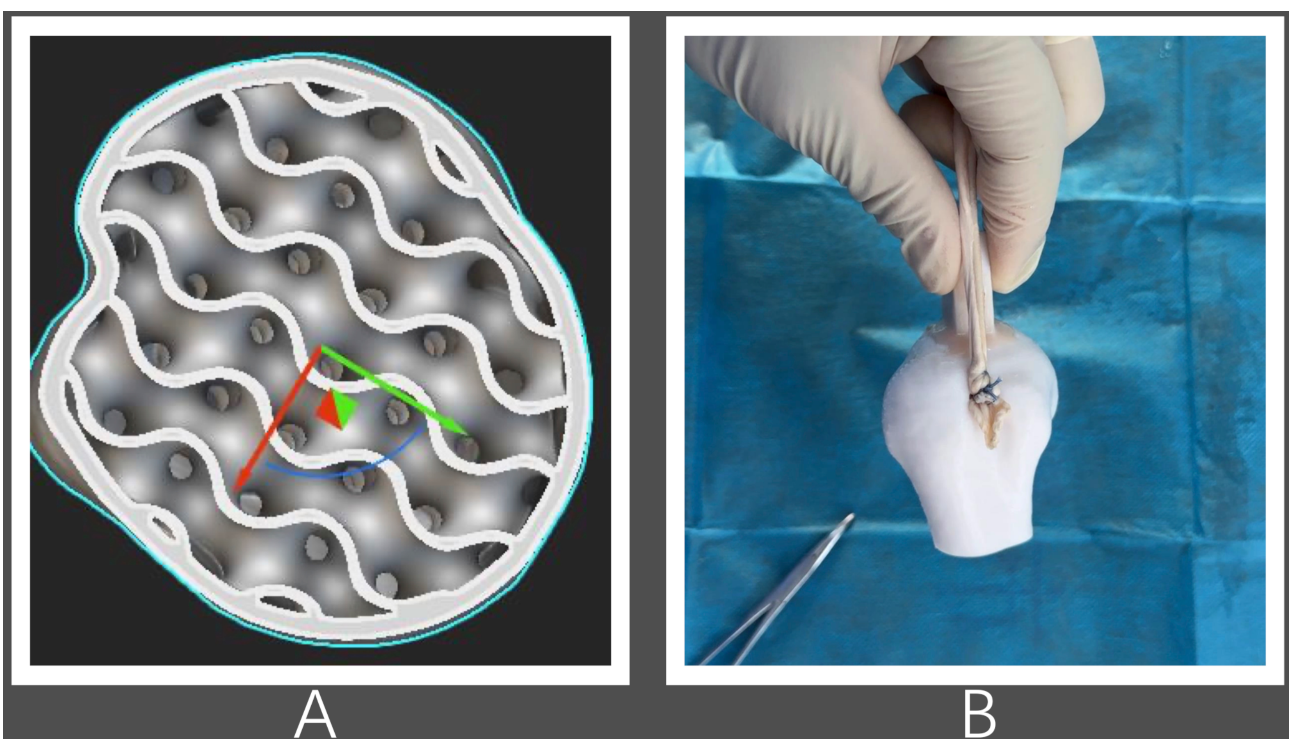

Fig. 1 (**A**) Axial view of the internal pattern in the 3D-printed humerus. (**B**) The knotted onlay tenodesis model with the single lasso loop suture anchor

Fig. 2 Diameter of the harvested tendon measured using the Vernier caliper

groups. These findings suggest that while the SLL technique provides comparable ultimate failure strength and displacement, it results in lower stiffness, which may be advantageous in reducing the risk of tendon migration and subsequent complications such as Popeye deformity.

The use of polylactic acid (PLA) in 3D printing has shown promising potential for creating bone models for biomechanical studies. PLA is an attractive material due to its biocompatibility, cost-effectiveness, and ease of use, making it accessible for both research and clinical applications. The study by Metzner et al. [14] demonstrated that PLA-based models, when combined with advanced printing techniques such as fused filament fabrication (FFF), can effectively replicate the mechanical behavior of cancellous bone. This finding aligns with other research efforts, such as those by Weinschenk et al. [15]. and Nägl et al. [16], which have shown that PLA can closely emulate the flexural properties of human femoral bones. These studies highlight the potential of PLA 3D printed bones as a viable alternative to traditional cadaveric specimens or synthetic bones, which are often limited by cost, availability, and variability. One of the key challenges in replicating bone models is capturing the anisotropic and inhomogeneous nature of bone tissue. Metzner et al. [14]

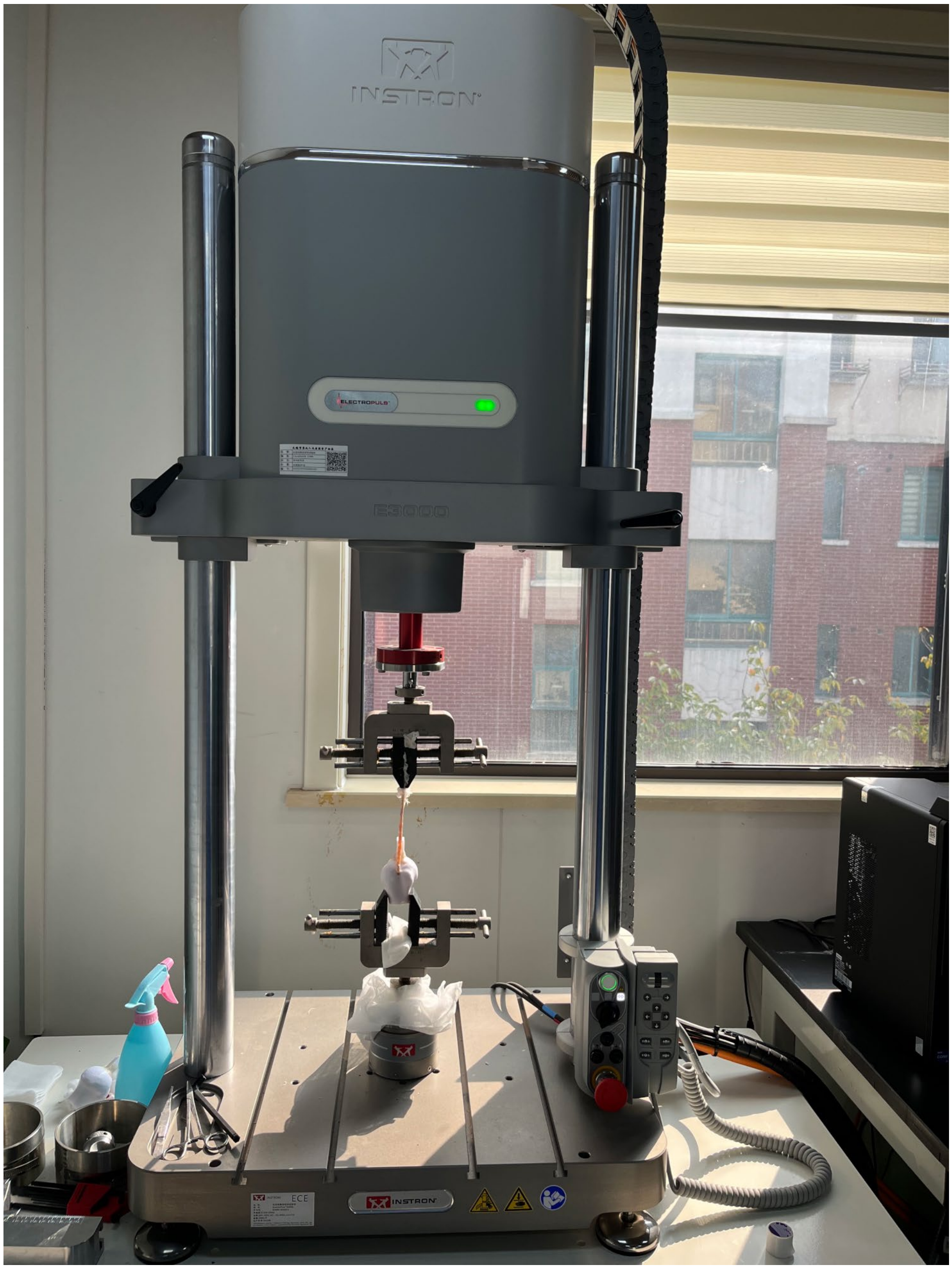

Fig. 3 Set up for biomechanical testing. The tendon was kept moist by spraying saline

Table 1 Comparison of Biomechanical outcomes between groups

	SLL	WSA	*P*-value
Diameter (mm)	6.35 ± 0.84	6.49 ± 0.64	0.73
Cycle 1 displacement (mm)	6.02 ± 3.23	4.61 ± 1.27	0.41
Cycle 500 displacement (mm)	9.66 ± 3.39	9.61 ± 4.14	0.80
Failure displacement (mm)	14.66 ± 4.70	16.58 ± 4.09	0.37
Ultimate failure load (N)	191.43 ± 42.59	188.57 ± 50.14	0.91
Stiffness (N/mm)	58.02 ± 5.62	72.24 ± 15.63	0.043

NOTE. No difference was observed in any of the parameters tested, except stiffness, between the two groups

SSL: single lasso loop; WSA: whipstitch with knotless suture anchor

addressed this by using a gyroid structure in their PLA models, which mimics the trabecular architecture of cancellous bone. The anisotropy of the PLA models was evaluated by comparing mechanical properties in different spatial directions, revealing a degree of anisotropy ranging from 1.2 to 3.0. This range is comparable to that observed in human cancellous bone, suggesting that PLA models can effectively replicate the directional mechanical behavior of bone. The ability to create models with varying infill densities further allows for the simulation of bone inhomogeneity, which is crucial for accurate biomechanical studies.The findings of this study are consistent

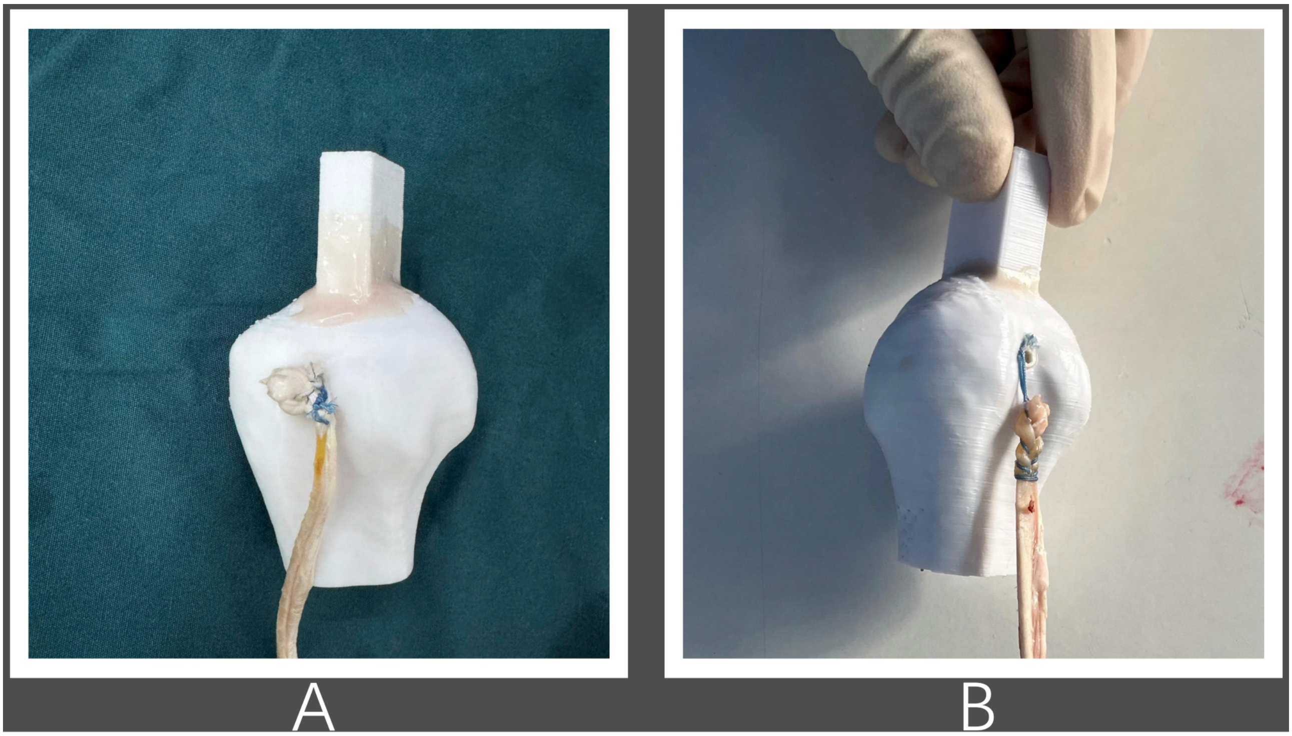

Fig. 4 Construct appearance after testing. (**A**) Knotted SLL tenodesis: an almost intact construct is observed. (**B**) Knotless WSA tenodesis: shows tendon migration and binding with no suture pull out

with previous research [11] demonstrating the potential of PLA-based models for orthopedic biomechanical studies. The use of a gyroid infill structure in the 3D printed models effectively mimics the trabecular architecture of cancellous bone, providing a realistic simulation of bone mechanics.

The optimal treatment of the long head of the biceps tendon pathologies has gradually transformed from biceps tenotomy to tenodesis [17–19]. Historically, open tenodesis techniques have been preferred because of their simplicity and proven efficacy. However, with advancements in arthroscopic methods, the prevalence of arthroscopic biceps tenodesis has significantly increased owing to the lower rate of complications, such as muscle cramping and Popeye deformity [5, 11, 20]. For overhead throwing athletes, the biceps tendon is important due to its a crucial role in stress absorption and humeral head restriction functions [21]. Generally, according to metrics, such as the American Shoulder and Elbow Surgeons (ASES) score, the Constant score, average range of motion, postoperative stiffness, and rate of complications, both open and arthroscopic procedures exhibit excellent functional outcomes. Furthermore, the failure rates or incidence of Popeye deformity do not differ significantly across the two techniques. However, considering the larger incisions required for open tendon fixation, scar size may be a decisive factor for patients opting for fixation over tenotomy for aesthetic reasons [22]. Additionally, arthroscopic suprapectoral tenodesis may result in a swifter recovery than open subpectoral tenodesis [23]. Despite high satisfaction rates in revision subpectoral biceps tenodesis,[20] some pain persisted in a significant number of patients; however, this residual pain pathology is difficult to assess.

Common tenodesis sites include the articular margin [24], suprapectoral [25], and subpectoral [26] locations. Moon et al. have reported that most intra-articular biceps tears may manifest a “hidden lesion” beyond the bicipital groove, extending to the distal extra-articular portion, which can be removed by open subpectoral tenodesis. Thus, they proposed that the subpectoral location may be regarded as the optimal tenodesis site for the absolute removal of all “hidden lesions” [27]. Various fixation methods, such as inlay and onlay techniques, have been proposed. Proponents of the traditional interference screw inlay tenodesis technique, argue that it allows for greater surface area contact between the tendon and cancellous bone by securing the tendon within a bony tunnel, facilitating the interaction with bone marrow-derived stem cells [28, 29]. However, this method may cause friction at the point where the tendon bends into the tunnel—a phenomenon often referred to as the “killer turn”—which can potentially lead to localized tendon wear [30]. Tan and colleagues used a rabbit biceps tendon fixation model to evaluate tendon healing within the bone tunnel, compared to its healing on the cortical surface. Histological analyses revealed comparable healing outcomes for tendons fixed within a bone tunnel and those on the cortical surface [31]. Consequently, the authors concluded that, given the similarities in histological healing quality and biomechanical integrity between the two methods, creating a large bone tunnel might be unnecessary as it could increase stress and fracture risk [31].

A series of 1083 patients underwent arthroscopic tenodesis studies with the inlay technique high in the groove, with an overall revision rate of 4.1%, including 0.4% biceps intervention [24], demonstrating its safety when treating arthroscopically. Guerra et al. found that suprapectoral and articular margin tenodesis have similar patient-reported outcome measures (PROMs), minimal clinically important difference (MCID), visual analog scale (VAS), American Shoulder and Elbow Surgeons (ASES), or single assessment numeric evaluation (SANE) scores at any time point, up to 2 years [32]. Chiang et al. have demonstrated that all-suture anchor and interference screws possess a comparable failure load and stiffness [33]. Similarly, Tashjian and Henninger conducted a comparative analysis and proposed that, while the failure load was akin for both all-suture and interference screw anchors, the interference screw exhibited greater stiffness [34]. Moreover, Golish et al. revealed that interference screws surpass all-suture anchors in both failure load and stiffness [35]. However, the inlay technique conducted with an interference screw led to a higher rate of Popeye deformity compared with the onlay knotless technique [5].

Common tendon preparation methods are whipstitch and Krackow; both approaches have demonstrated their sound mechanical properties [36–39]. Although the suture type or technique has little influence on the outcome after acute lower-extremity tendon rupture repair [40], their effects remain unknown in the upper extremities, such as biceps tenodesis. One of the reasons for a preference for whipstitch was its slightly higher ultimate strength and lower stiffness [41]. Furthermore, we found it is less time-consuming compared with the Krackow stitch, based on our practices. While executing biceps tendon stump knotless onlay tenodesis, the preparatory procedure for extracorporeal suture can be notably intricate. The SLL, initially introduced for biceps tenodesis in rotator cuff repair [6], has since evolved into the 360° lasso loop method, which is applied to the tenodesis region [7]. This advancement offers increased convenience by eliminating the need for tendon preparation in arthroscopic procedures. Despite the lasso loop's ability to achieve a higher ultimate failure load and stiffness, the augmented stiffness of the 360° lasso loop may elevate the risk of tendon damage due to "potential cutting," which may be a reason for postoperative Popeye deformity [7].

The knotless suture anchor has a higher stiffness than suture anchors, including titanium and all other suture anchors [42, 43]. Although, no significant displacement and ultimate load effects were found, our study indicates that the knotless onlay technique exhibits increased stiffness compared to the SLL technique. In all seven models analyzed, the braided tendons were observed to undergo tight binding and deformation. This phenomenon is likely associated with the "potential cutting" effects, depicted as tendon migration [44], which is also considered the failure mode [45]. Therefore, the lower stiffness of the SLL onlay technique may lead to reduced tendon migration, thereby posing less risk for fixation failure.

Limitations

The present study has some limitations. First, bone mineral density and the architecture of the trabecular layer were not realistically reconstructed; instead, an artificial gyroid arrangement was used. Second, the 3D-printed model, used in our study, was not benchmarked against cadaveric bone samples with normal bone mineral density. Further studies are needed to evaluate its biomechanical properties compared with the human humerus.

Conclusion

Compared with WSA onlay tenodesis technique, the SLL technique has a similar ultimate failure load and cyclic load displacement but a lower stiffness, which may result in less complexity and a potentially lower rate of tendon migration. Thus, SLL biceps tenodesis may be preferred for arthroscopic biceps tenodesis.

Supplementary Information

The online version contains supplementary material available at https://doi.org/10.1186/s13018-025-05757-5.

Supplementary Video 1: The apparent construct failure mode of the SLL by the knot breaking out during the failure load test

Supplementary Video 2: Typical failure mode of WSA tenodesis. The suture tightly binds the tendon and is pulled out from the knotless anchor during the failure load test

Acknowledgements
None.

Author contributions
Study conception and design: JY; Grant funding application: JY and JYM; Research ethics board application and maintenance: JY and JYM; Data collection: JY, KH, and RFQ; Writing of the paper: JY; Reviewing and approval of the paper: JY and JYM. The authors read and approved the final manuscript.

Funding
This study received funding from the Wuxi Municipal Health Commission Youth Project (Grant Number: Q202460); Duo-Innovative and Excellent Doctors Project of Wuxi Ninth People's Hospital (2021) (Grant Number:YB202111). Shanghai Key Laboratory of Peripheral Nerve and Microsurgery (20DZ2270200), "Top Medical Team" of Wuxi Taihu Talent Plan (2023).

Data availability

No datasets were generated or analysed during the current study.

Declarations

Competing interests

The authors declare no competing interests.

Received: 22 February 2025 / Accepted: 25 March 2025
Published online: 07 April 2025

References

1. Frantz TL, Shacklett AG, Martin AS, Barlow JD, Jones GL, Neviaser AS, Cvetanovich GL. Biceps tenodesis for superior labrum Anterior-Posterior tear in the overhead athlete: A systematic review. Am J Sports Med. 2021;49:522–8.
2. Lorentz NA, Hurley ET, Colasanti CA, Markus DH, Alaia MJ, Campbell KA, Strauss EJ, Jazrawi LM. Return to play after biceps tenodesis for isolated SLAP tears in overhead athletes. Am J Sports Med. 2022;50:1369–74.
3. Shin MH, Baek S, Kim TM, Kim H, Oh KS, Chung SW. Biceps tenodesis versus superior labral anterior and posterior (SLAP) lesion repair for the treatment of SLAP lesion in overhead athletes: A systematic review and Meta-analysis. Am J Sports Med. 2022;50:3987–97.
4. Recker AJ, Waters TL, Bullock G, Rosas S, Scholten DJ 2nd, Nicholson K, Waterman BR. Biceps tenodesis has greater expected value than repair for isolated type II SLAP tears: A Meta-analysis and expected-Value decision analysis. Arthroscopy. 2022;38:2887–e28962884.
5. Haidamous G, Noyes MP, Denard PJ. Arthroscopic biceps tenodesis outcomes: A comparison of inlay and onlay techniques. Am J Sports Med. 2020;48:3051–6.
6. Lafosse L, Van Raebroeckx A, Brzoska R. A new technique to improve tissue grip:the lasso-loop stitch. Arthroscopy: J Arthroscopic Relat Surg. 2006;22:1246. e1241-1246. e1243.
7. Muller S, Flury R, Zimmermann S, de Wild M, Fogerty S, Lafosse L, Bongiorno V, Rosso C. The new LassoLoop360 degrees technique for biomechanically superior tissue grip. Knee Surg Sports Traumatol Arthrosc. 2019;27:3962–9.
8. Chen D, Zhang Q, Deng J, Cai Y, Huang J, Li F, Xiong K. A shortage of cadavers: the predicament of regional anatomy education in Mainland China. Anat Sci Educ. 2018;11:397–402.
9. Ma A, Ding Y, Lu J, Wo Y, Ding W. An examination of the status, contexts of anatomical body donation, and perspectives in China. Ann Anat. 2024;253:152230.
10. Weinschenk RC, Oldham BM, Nagaraja KM, Alam F, Samade R, Li W. Three-dimensional-printed femoral diaphysis for Biomechanical testing—Optimization and validation. J Orthop Research® 2024.
11. Ock J, Seo J, Koh KH, Kim N. Comparing the Biomechanical properties of conventional suture and all-suture anchors using patient-specific and realistic osteoporotic and non-osteoporotic Phantom using 3D printing. Sci Rep. 2023;13:20976.
12. Lafosse L, Van Raebroeckx A, Brzoska R. A new technique to improve tissue grip: the lasso-loop stitch. Arthroscopy. 2006;22:e12461241–1243.
13. Prodromos CC, Hecker A, Joyce B, Finkle S, Shi K. Elongation of simulated whipstitch post anterior cruciate ligament reconstruction tibial fixation after Cyclic loading. Knee Surg Sports Traumatol Arthrosc. 2009;17:914–9.
14. Metzner F, Neupetsch C, Carabello A, Pietsch M, Wendler T. Drossel W-G: Biomechanical validation of additively manufactured artificial femoral bones. BMC Biomedical Eng. 2022;4:6.
15. Weinschenk RC, Oldham BM, Nagaraja KM, Alam F, Samade R, Li W. Three-dimensional-printed femoral diaphysis for Biomechanical testing—Optimization and validation. J Orthop Research®. 2024;42:2735–42.
16. Nägl K, Reisinger A, Pahr DH. The biomechanical behavior of 3D printed human femoral bones based on generic and patient-specific geometries. 3D printing in medicine. 2022;8:35.
17. Lädermann A. Editorial commentary: the long head of the biceps tendon is useful for shoulder reconstruction including glenohumeral stabilization: from biceps killers to biceps users. Volume 39. Elsevier; 2023. pp. 202–3.
18. Werner BC, Brockmeier SF, Gwathmey FW. Trends in long head biceps tenodesis. Am J Sports Med. 2015;43:570–8.
19. Erickson BJ, Jain A, Abrams GD, Nicholson GP, Cole BJ, Romeo AA, Verma NN. SLAP lesions: trends in treatment. Arthroscopy: J Arthroscopic Relat Surg. 2016;32:976–81.
20. Slenker NR, Lawson K, Ciccotti MG, Dodson CC, Cohen SB. Biceps tenotomy versus tenodesis: clinical outcomes. Arthroscopy: J Arthroscopic Relat Surg. 2012;28:576–82.
21. Yu J, Yin Y, Chen W, Mi J. Long head of the biceps tendon plays a role in stress absorption and humeral head restriction during the late cocking and deceleration phases of overhead throwing: A finite element study. J Shoulder Elbow Surg 2024.
22. Forsythe B, Zuke WA, Agarwalla A, Puzzitiello RN, Garcia GH, Cvetanovich GL, Yanke AB, Verma NN, Romeo AA. Arthroscopic suprapectoral and open subpectoral biceps Tenodeses produce similar outcomes: a randomized prospective analysis. Arthroscopy: J Arthroscopic Relat Surg. 2020;36:23–32.
23. Ahn J, Kim J-H, Shin S-J. Arthroscopic suprapectoral biceps tenodesis provided earlier shoulder function restoration compared with open subpectoral biceps tenodesis during the recovery phase. J Shoulder Elbow Surg. 2024;33:678–85.
24. Brady PC, Narbona P, Adams CR, Huberty D, Parten P, Hartzler RU, Arrigoni P, Burkhart SS. Arthroscopic proximal biceps tenodesis at the articular margin: evaluation of outcomes, complications, and revision rate. Arthroscopy: J Arthroscopic Relat Surg. 2015;31:470–6.
25. Pratte T, Smith T, Arevalo A, Wazen J, Rubenstein D. Arthroscopic suprapectoral biceps tenodesis: the best of both worlds. Arthrosc Techniques. 2022;11:e1619–23.
26. Hoffer AJ, Tokish JM. Arthroscopic subpectoral tenodesis of the long head of the biceps brachii. Arthrosc Techniques 2024:103079.
27. Moon SC, Cho NS, Rhee YG. Analysis of hidden lesions of the extra-articular biceps after subpectoral biceps tenodesis: the subpectoral portion as the optimal tenodesis site. Am J Sports Med. 2015;43:63–8.
28. Wang D, Tan H, Lebaschi AH, Hutchinson ID, Ying L, Deng X-H, Rodeo SA, Warren RF. Comparison of bone tunnel and cortical surface Tendon-to-Bone healing in a rabbit biceps tenodesis model. J Shoulder Elbow Surg. 2018;27:e136–7.
29. Soon MY, Hassan A, Hui JH, Goh JC, Lee E. An analysis of soft tissue allograft anterior cruciate ligament reconstruction in a rabbit model: a short-term study of the use of mesenchymal stem cells to enhance tendon osteointegration. Am J Sports Med. 2007;35:962–71.
30. Silva MJ, Thomopoulos S, Kusano N, Zaegel MA, Harwood FL, Matsuzaki H, Havlioglu N, Dovan TT, Amiel D, Gelberman RH. Early healing of flexor tendon insertion site injuries: tunnel repair is mechanically and histologically inferior to surface repair in a canine model. J Orthop Res. 2006;24:990–1000.
31. Tan H, Wang D, Lebaschi AH, Hutchinson ID, Ying L, Deng XH, Rodeo SA, Warren RF. Comparison of bone tunnel and cortical surface Tendon-to-Bone healing in a rabbit model of biceps tenodesis. J Bone Joint Surg Am. 2018;100:479–86.
32. Guerra JJ, Curran GC, Guerra LM. Subpectoral, suprapectoral, and top-of-groove biceps tenodesis procedures lead to similar good clinical outcomes: comparison of biceps tenodesis procedures. Arthrosc Sports Med Rehabilitation. 2023;5:e663–70.
33. Chiang FL, Hong C-K, Chang C-H, Lin C-L, Jou I-M, Su W-R. Biomechanical comparison of all-suture anchor fixation and interference screw technique for subpectoral biceps tenodesis. Arthroscopy: J Arthroscopic Relat Surg. 2016;32:1247–52.
34. Tashjian RZ, Henninger HB. Biomechanical evaluation of subpectoral biceps tenodesis: dual suture anchor versus interference screw fixation. J Shoulder Elbow Surg. 2013;22:1408–12.
35. Golish SR, Caldwell PE III, Miller MD, Singanamala N, Ranawat AS, Treme G, Pearson SE, Costic R, Sekiya JK. Interference screw versus suture anchor fixation for subpectoral tenodesis of the proximal biceps tendon: a cadaveric study. Arthroscopy: J Arthroscopic Relat Surg. 2008;24:1103–8.
36. Agarwalla A, Puzzitiello RN, Leong NL, Shewman EF, Verma NN, Romeo AA, Forsythe B. A Biomechanical comparison of two arthroscopic suture techniques in biceps tenodesis: whip-stitch vs. simple suture techniques. J Shoulder Elbow Surg. 2019;28:1531–6.
37. da Assunção RE, Haddad R, Bruce WJ, Walker P, Walsh WR. Whip stitch versus grasping suture for tendon autograft. Eur J Orthop Surg Traumatol. 2013;23:105–9.
38. Spiegl UJ, Smith SD, Euler SA, Millett PJ, Wijdicks CA. Biomechanical consequences of proximal biceps tenodesis stitch location: musculotendinous junction versus tendon only. Knee Surg Sports Traumatol Arthrosc. 2015;23:2661–6.

39. Hahn JM, İnceoğlu S, Wongworawat MD. Biomechanical comparison of Krackow locking stitch versus nonlocking loop stitch with varying number of throws. Am J Sports Med. 2014;42:3003–8.
40. Barber FA. Editorial commentary: suture type or technique has little influence on outcome after acute Lower-Extremity tendon rupture. Volume 37. Elsevier; 2021. pp. 2934–6.
41. Diaz MA, Branch EA, Dunn JG, Brothers A, Jordan SE. Whipstitch and locking stitch show equivalent elongation and load to failure across 3 suture systems in a Biomechanical model of quadriceps tendon grafts for anterior cruciate ligament reconstruction. Arthrosc Sports Med Rehabilitation. 2024;6:100968.
42. Deichsel A, Rolf J, Raschke MJ, Milstrey A, Klimek M, Peez C, Herbst E, Kittl C. Knotless suture anchors display favorable elongation but an inferior ultimate failure load versus titanium suture anchors and All-Suture anchors: A Biomechanical comparison in a Porcine model. Orthop J Sports Med. 2024;12:23259671241300520.
43. Johns WL, Baumann AN, Callaghan ME, Walley KC, Patel NK, Salvo J. Knotless versus knotted suture anchors for labral repair of the hip: A systematic review of clinical and Biomechanical outcomes. Am J Sports Med 2025:03635465241239689.
44. Forsythe B, Berlinberg EJ, Khazi-Syed D, Patel HH, Forlenza EM, Okoroha KR, Williams BT, Yanke AB, Cole BJ, Verma NN. Greater postoperative biceps tendon migration after arthroscopic suprapectoral or open subpectoral biceps tenodesis correlates with lower patient-reported outcome scores. Arthroscopy: J Arthroscopic Relat Surg 2024.
45. Hsu K-L, Su W-R. Editorial commentary failure following biceps long head tenodesis includes Popeye sign, cramping, and tendon migration. Elsevier; 2024.

Publisher's note